fortune Journals

Research Article

JOURNAL OF RADIOLOGY AND CLINICAL IMAGING

ISSN: 2644-2809

ADC Mapping With 12 b Values: Can We Improve Image Quality In The Diffusion Sequence of Prostate MRI?

Lucas Scatigno Saad[1*], George De Queiroz Rosas[2], Homero José De Farias E Melo[3], Jacob Szejnfeld

Abstract

Introduction: Prostate cancer (PCa) is one of the most prevalent tumors in male population. Multiparametric magnetic resonance imaging (mp-MRI) of the prostate is of great importance in the diagnosis of PCa, with particular emphasis on diffusion-weighted sequences. Nevertheless, diffusion-weighted imaging (DWI) sometimes exhibits limited definition and sharpness, hindering characterization of suspect lesions and normal anatomy. To address this challenge in obtaining clearer images, was developed a DWI protocol with 12 b values.

Objectives: To compare the sharpness and conspicuity of images obtained by DWI sequences with 4 versus 12 b values in the detection of PCa by mp-MRI. Secondarily, to validate the use of this new sequence in clinical practice by quantitative and comparative analysis of apparent diffusion coefficient (ADC) values, and correlate ADC values with the PI-RADS classification and Gleason score of identified tumors.

Methods: A total of 158 mp-MRI scans were evaluated. In all scans, two diffusion sequences were performed, with 4 and 12 b values, and ADC maps were calculated for each (ADC_4 and ADC_{12} respectively). Individual and comparative analyses of image sharpness and quality were done, followed by assessment of correlation with PI-RADS. A sensitivity comparison was also performed for the diagnosis of PCa and the degree of tumor differentiation (Gleason score).

Results: Mean ADC_4 and ADC_{12} values in normal tissues (ADC_4, 1793.3×10-6 mm2/s; ADC_{12}, 1100×10-6 mm2/s) were significantly higher than in areas of tumor (ADC_4, 1105.9×10-6 mm2/s; ADC_{12}, 689.4×10-6 mm2/s) ($p<0.001$). ADC values correlated well with the PI-RADS classification, distinguishing scores 3, 4 and 5 and with ADC tending to decline as the Gleason grade (tumor aggressiveness) increased. The conspicuity of the images obtained on ADC_{12} maps was consistent with greater sharpness compared to ADC_4 maps, with high inter-observer agreement and statistical relevance.

Conclusions: Diffusion images obtained with 12 b values (ADC_{12}) provide superior quality and conspicuity for the diagnosis of prostate cancer and correlate well with the PI-RADS classification and Gleason grade of biopsy specimens.

Keywords: Image analysis; Artificial intelligence; Machine learning; Computed tomography.

Introduction

Prostate cancer was the second most frequently diagnosed cancer and the

Affiliation:

[1]Universidade Federal de São Paulo (UNIFESP). Rua Sena Madureira, 1500, Vila Clementino, 04021-001, São Paulo, SP, Brazil. ORCID: 0000-0002-8203-1251.

[2]Universidade Federal de São Paulo (UNIFESP). Rua Sena Madureira, 1500, Vila Clementino, 04021-001, São Paulo, SP, Brazil. ORCID: 0000-0001-6939-7112.

[3]Universidade Federal de São Paulo (UNIFESP). Rua Sena Madureira, 1500, Vila Clementino, 04021-001, São Paulo, SP, Brazil. ORCID: 0000-0002-5287-9294.

[4]Universidade Federal de São Paulo (UNIFESP). Rua Sena Madureira, 1500, Vila Clementino, 04021-001, São Paulo, SP, Brazil. ORCID: 0000-0002-6145-0529.

Corresponding author:
Lucas Scatigno Saad, Rua Jaspe, 32, Aclimacao 01531-060 - Sao Paulo, SP – Brazil.

E-mail: lucsaad@gmail.com

Citation: Lucas Scatigno Saad, George De Queiroz Rosas, Homero José De Farias E Melo, Jacob Szejnfeld. ADC Mapping With 12 b Values: Can We Improve Image Quality In The Diffusion Sequence of Prostate MRI?. Journal of Radiology and Clinical Imaging. 6 (2023): 16-23.

Received: January 07, 2023
Accepted: January 19, 2023
Published: February 01 2023

Saad LS, et al., J Radiol Clin Imaging 2023
DOI:10.26502/jrci.2809067

fifth cause of death by cancer in the male population over the world in 2020 [1].

Magnetic resonance imaging (MRI) for evaluation of the prostate entered clinical use in the mid-1980s [2-3], with the objective of staging already diagnosed tumors. Major technological advances in the field have made it possible to explore the potential of this method for detecting suspicious lesions as well.

Diffusion-weighted imaging (DWI) is a functional MRI sequence that measures the signal resulting from the movement of water molecules within tissues. DWI can be substantially useful as an adjunct to diagnosis of PCa, with particular importance since the advent of PI-RADS version 2 and mainly for tumors in the peripheral zone, having become a key sequence to determine the presence and severity of focal lesions [4-5].

Diffusion sequences can be obtained using at least two different b values, that demonstrate different ranges of motion of the targeted molecules. This signal difference is calculated by a first-degree exponential equation that yields the apparent diffusion coefficient (ADC). The ADC is expressed in square millimeters per second (mm2/s). It is a reproducible measurement of diffusion which can be obtained on any workstation by drawing a region of interest (ROI) and generates the ADC map image.

The correlation between numerical ADC values and the aggressiveness of prostate tumors has been widely studied and documented in the literature [6-11]. Lesions with significant diffusion restriction (low ADC values) are associated with high histological aggressiveness as measured by the Gleason score and, therefore, can correlate with prognosis and treatment planning for these patients [7-8-9].

Prostate images obtained with high b values have excellent sensitivity to demonstrate lesions, at the expense of image distortion and loss of spatial resolution [10]. Other studies have reported overlap in ADC values in some situations; namely, those obtained from diffusion sequences with b values up to 1000 s/mm2 may represent either normal or neoplastic tissue [11-12]. There is also no consensus in the current literature as to which and how many different b values should be used for MRI of the prostate between different protocols and equipment [13-14].

This technical limitation of DWI motivated the search for improvements, particularly with the objective of improving image resolution. Imaging protocols have been developed to analyze the behavior of the normal prostate and suspicious lesions on sequences with distinct types and numbers of b values. Among these, increasing the number of b values acquired to 12 appeared to be particularly helpful.

The need to validate the diagnostic utility of this new technique prompted to conduct this study, which is based on a qualitative and quantitative comparison of the new technique with that used in the standard routine MRI of the prostate.

Diffusion-weighted imaging is a key component of mp-MRI and fulfills the appropriate criteria for the diagnosis of PCa. However, diffusion images and ADC maps sometimes have limited resolution, making it difficult to properly assess the prostate and identify lesions. To improve the quality of visualization and anatomical definition of diffusion sequences without losing its primary (diagnostic) capacity, a new protocol was developed, with acquisition of 12 increasing b values to compare it with the standard 4 b value diffusion technique used in the routine protocol of prostate mp-MRI. The key objectives of this study were:

1. to compare the sharpness and conspicuity of images obtained by DWI sequences with 4 versus 12 b values in evaluation of the normal prostate and for characterization of suspicious lesions; and
2. to establish the relationship between ADC measures generated by the two techniques and assess their correlation with Gleason grades.

Material and Methods

Case series

Prostate mp-MRI scans performed on 162 patients with clinical or laboratory indications for PCa testing were evaluated. The study sample comprised patients with a clinically significant increase in PSA and/or abnormal digital rectal examination performed for cancer screening, as well as patients with confirmed PCa who underwent MRI for tumor staging. All scans were carried out from a specialized diagnostic medicine center. Due to corrupted files or lost images reported by de PACS system, 4 patients had to be excluded from de analysis.

Technical Parameters

Image acquisition was performed in 3-Tesla scanners with a 45 mT/m gradient (Magnetom Verio and Magnetom Skyra; Siemens Medical Systems, Erlangen, Germany), using a standard torso coil.

The sequences performed are shown in Table 1 and described below: axial T2 spin-echo, coronal and sagittal, for assessment of prostate morphology (256 x 230 matrix, slice thickness 3.0 mm, FOV 160 x 160 mm, TR = 3560 ms, TE = 114 ms), and axial T1 spin-echo (256 x 230 matrix, slice thickness 3.0 mm, FOV 160 x 160 mm, TR = 550 ms, TE = 9.5 ms).

Two diffusion weighted gradient sequences (128 x 128 matrix, slice thickness 3.0 mm, FOV 240 x 240 mm) were employed for functional assessment of the prostate: diffusion 4 (four b values = 0, 100, 400, and 1000 s/mm2) and diffusion 12 (twelve b values = 0, 50, 100, 150, 300, 600, 900, 1200, 1500, 1800, 2100, and 2400 s/mm2).

Saad LS, et al., J Radiol Clin Imaging 2023
DOI:10.26502/jrci.2809067

Table 1: MRI sequences performed in the study protocol.

Sequence	Thickness (mm)	FOV (mm)	TR (ms)	TE (ms)	Matrix	b (s/mm2)
Sagittal T2	3	160	3,790	114	256 x 204	
Axial T2	3	150	3,930	124	256 x 230	
Coronal T2	3	160	3,560	114	256 x 230	
Axial T1	3	150	550	9.5	256 x 230	
Axial T2 FS	3	150	5,200	134	256 x 204	
Diffusion ($ADC_{4)}$	3	240	5,500	75	128 x 128	0; 100; 400; 1000
Diffusion (ADC_{12})	3	250	5,900	72	128 x 128	0; 50; 100; 150; 300; 600; 900; 1200; 1500; 1800; 2100; 2400
T2_haste_AXIAL Pelvis	5	320	1,500	96	320 x 260	
Axial In-Out Phase	2.8	377	3.51	1.1	256 x 256	
T1_vibe_fs_cor_p2_bh_384	1.5	350	3.92	1.62	512 x 332	
T1 VIBE fs ax bh P2 spair	1.7	330	3.17	1.59	320 x 224	
Perfusion Axial	1.6	200	3.81	1.53	288 x 172	
T1_vibe_fs_cor -Pgd	1.5	350	3.92	1.62	512 x 332	

Except in patients with absolute contraindications, the standard protocol included dynamic pre- and post-contrast enhancement images.

Post-processing was then performed to calculate ADC maps with 4 b values (ADC_4) and with 12 b values (ADC_{12}), using a first-degree exponential equation model.

Analysis of Imaging Findings

Images from morphology and functional sequences were evaluated synchronously and simultaneously on a dedicated workstation (syngo.via™, Siemens) and analyzed by a radiologist with expertise in prostate imaging. The imaging criteria for a clinically significant prostatic lesion (suspicion for cancer) in the peripheral zone were those described in PI-RADS version 2 [5].

Measurements of ADC_4 and ADC_{12} values were performed using the region of interest (ROI) tool in areas identified as suspicious, allowing for the largest possible lesion area and copying the same area to the ADC_4 and ADC_{12} maps (Figure 1), through a specific tool that duplicated the ROI measurement for the sequence of interest. In the absence of a lesion, measurements were performed only on areas of normal prostate tissue in the peripheral zone.

To assess image quality on the ADC maps, all scans were anonymized, randomly ordered for both sequences, and analyzed by two observers. Image quality for anatomical evaluation and lesion identification was scored on a Likert scale from 1 (very low sharpness) to 5 (excellent sharpness). Images were classified for sharpness and conspicuity in the following parameters: anatomy

of the prostate and visualization of the lesion (when present). To assess anatomy, the parameters were visualization of margins, ability to differentiate between the different zones

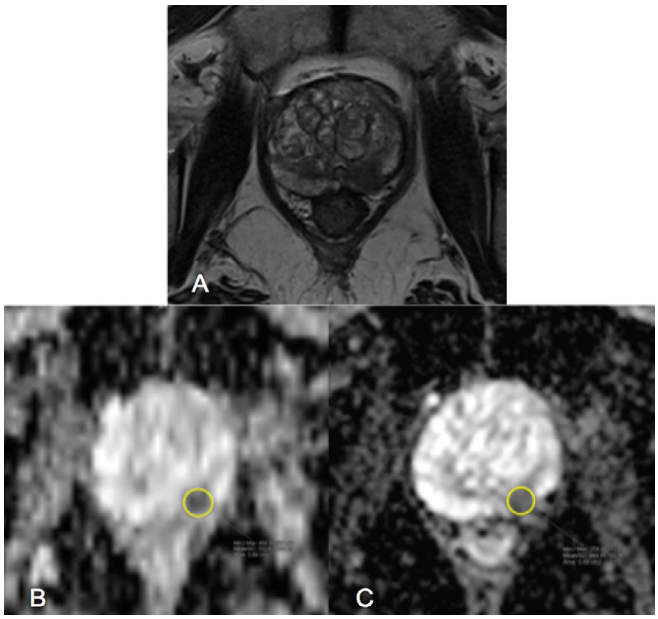

Figure 1: Representative magnetic resonance imaging in patient with a prostate lesion

Magnetic resonance imaging of the prostate in a patient with a suspicious lesion. **A)** T2 sequence showing the morphological appearance of the lesion in the left peripheral zone. **B)** ADC_4; lesion with diffusion restriction. Yellow circle denotes the measurement performed through the ROI tool. **C)** ADC_{12}; lesion with diffusion restriction. Yellow circle denotes the measurement performed through the ROI tool.

of the prostate, and its relationship to adjacent structures. When a suspicious lesion was present, the criteria of interest were its location and margins.

Statistical Analysis

Means, medians, and standard deviations of the ROI measurements of ADC_4 and ADC_{12} were calculated for

Saad LS, et al., J Radiol Clin Imaging 2023
DOI:10.26502/jrci.2809067

normal areas and lesion areas. Student's t-test was used to compare signal behavior between normal and lesion areas. A regression model with Pearson correlation was used to compare measurements obtained in ADC_4 and in ADC_{12}. The mean ADC values were correlated with the Gleason score of the corresponding biopsy specimens, using dispersion models calculated by analysis of variance (ANOVA) and the Mann-Whitney U test, respectively. Receptor operating characteristic (ROC) curves were used to calculate the sensitivity and specificity of the parameters of interest for cancer prediction.

Regarding analysis of image quality, paired Wilcoxon tests were used for comparison between sequences and between observers, while the agreement between observer scores was calculated with Kendall's Tau-b coefficient.

Results

Overall, 50 patients had suspicions lesions (as defined by the mp-MRI clinically significant inclusion criteria) measurable by the study method. Normal areas were measured both in patients with and those without suspicious lesions, for a total of 158 patients.

Means, medians, standard deviations, and ranges are given in Table 2.

Means and medians were higher in normal areas and lower in lesion areas. Absolute ADC values were lower overall with the ADC_{12} sequence than with ADC_4, as shown by analysis of the range of values (min-max) obtained from each sequence.

Comparison between mean ADC_4 values for normal versus lesion areas showed significantly higher means in normal areas than in lesion areas (Student's t-test for paired samples, $p < 0.001$) (Figure 2). The same relationship was observed in ADC_{12} values, with significantly higher means in normal areas than in lesion areas, demonstrating similarity between the two techniques (Figure 3).

Table 2. ADC measurements obtained in ADC_4 and ADC_{12}

	Normal ADC_4	Lesion ADC_4	Normal ADC_{12}	Lesion ADC_{12}
Mean	1793.3	1105.9	1100	689.4
95% FI for mean				
Lower limit	1748.2	1022	1071.9	642.6
Upper limit	1838.3	1189.8	1128.1	736.1
Median	1829.5	1162	1092.5	680
Standard deviation	286.4	298.3	178.7	166.1
Minimum	1057	478	665	260
Maximum	2631	1695	1461	947

values expressed as 10^{-6} mm^2/s.

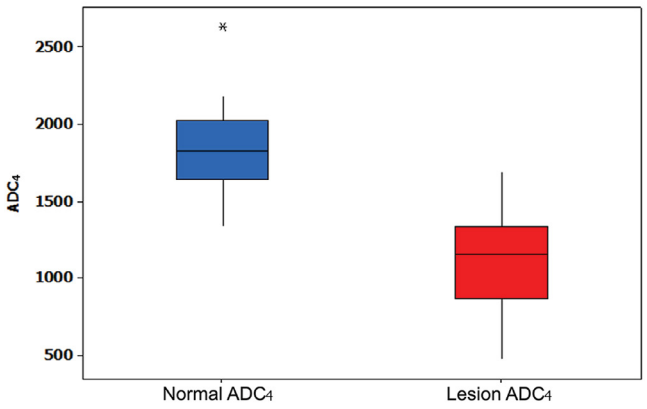

Figure 2: Box-plot of Normal ADC_4 and Lesion ADC_4

Box diagram showing ADC_4 values for normal areas (blue) higher than for lesion areas (red). $p < 0.001$. (Unit mm/s^2). ADC, apparent diffusion coefficient.

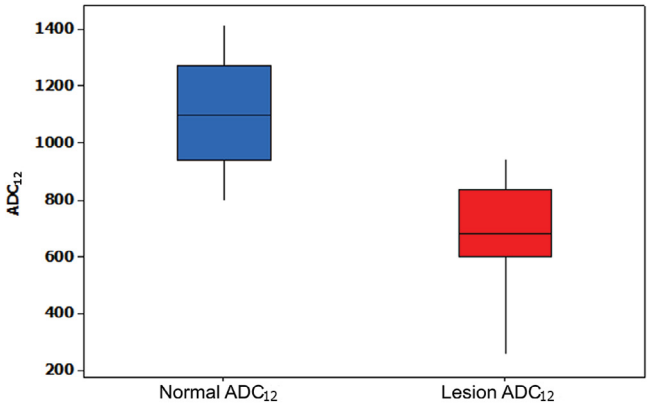

Figure 3: Box-plot of Normal ADC_{12} and Lesion ADC_{12}.

Box diagram showing ADC12 values for normal areas (blue) higher than for lesion areas (red). $p < 0.001$. (Unit mm/s2). ADC, apparent diffusion coefficient.

Given this similarity in behavior between the two maps, measurements were analyzed using a regression model between normal areas and lesion areas (Figure 4). This revealed a constant correlation between ADC_4 and ADC_{12} measurements in lesion areas, which yielded the following regression formula:

$$ADC_4Lesion = 1.528 * ADC_{12}Lesion$$

Using the same regression model, a similar correlation was observed between ADC_4 and ADC_{12} measurements in normal areas (Figure 5), yielding the following formula:

$$ADC_4Normal = 453.5 + 1.218 * ADC_{12}Normal$$

Of the 158 patients included, 52 underwent prostate biopsy, with the following results: cancer confirmed in 28 (53.8%), cancer ruled out in 14 (27.0%), prostatitis diagnosed

Saad LS, et al., J Radiol Clin Imaging 2023
DOI:10.26502/jrci.2809067

in 7 (13.4%), atypical small acinar proliferation in 2 (3.8%), and prostatic intraepithelial neoplasia in 1 (2.0%). Gleason scores for the patients with confirmed prostate neoplasm were as follows: 11 patients were Gleason 6, 10 patients were Gleason 7, 4 patients were Gleason 8, and 3 patients were Gleason 9. Gleason scores were pooled to facilitate analysis, with both 3 + 4 and 4 + 3 scores classified as Grade 7 and 4 + 5 and 5 + 4 classified as Grade 9. The mean ADC_4 and ADC_{12} values for the different Gleason grades are given in Table 3.

As shown in the table, mean ADC values decreased as the Gleason score increased; however, on analysis of correlation, these differences in were not statistically significant for differentiation of pathological grades ($p = 0.127$ for ADC_4, $p = 0.165$ for ADC_{12}). This demonstrates a trend towards lower ADC values with increasing pathological aggressiveness on both ADC maps.

Analysis of the predictive value of the ADC maps for the detection of confirmed PCa (through ROC curves and subsequent AUC calculation) showed that both were significantly predictive for cancer ($p < 0.05$); the ADC_4 map had a minimum cut-off value of 1153 x 10-6 mm^2/s, with AUC = 0.724 (95% CI 0.609-0.893), 71.5% sensitivity, and 72.3% specificity; the ADC_{12} map had a minimum cutoff value of 658.5 x 10^{-6} mm^2/s, AUC = 0.729 (95% CI 0.575-0.884), 71.4% sensitivity, and 70.6% specificity (Figure 6).

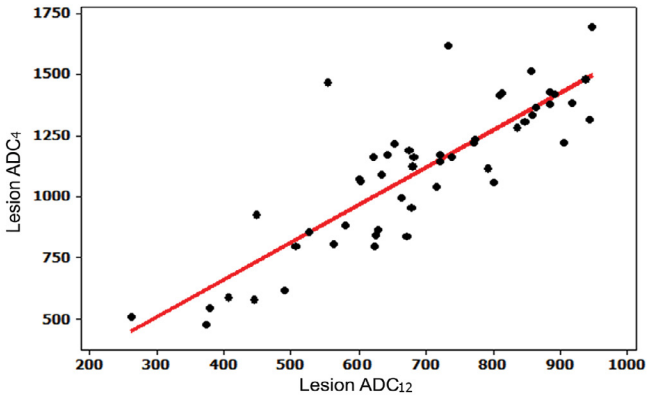

Figure 4: Scatter plot of ADC_4 and ADC_{12} values in lesion areas. (Unit mm/s^2).

Using the same regression model, a similar correlation was observed between ADC_4 and ADC_{12} measurements in normal areas (Figure 5), yielding the following formula:

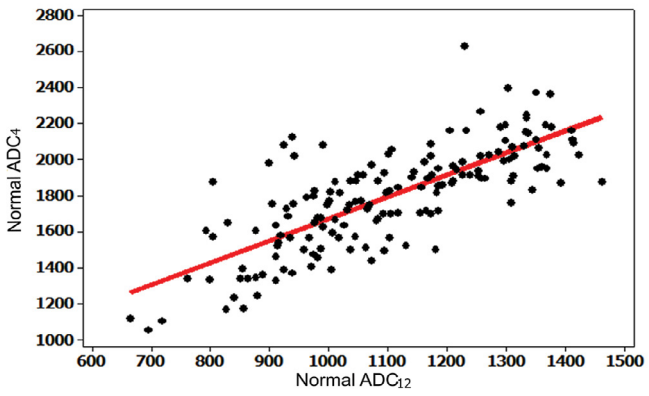

Figure 5: Scatter plot of ADC_4 and ADC_{12} values in normal tissue. (Unit mm/s^2)

The results of image quality evaluation, performed by two observers using a Likert scale from 1 to 5, are summarized in Table 4. The mean anatomical conspicuity score was 3.037 for ADC4 and 4.446 for ADC12. For lesion conspicuity, ADC4 had a mean score of 3.489, versus 3.826 for ADC12.

On comparative analysis between ADC_4 and ADC_{12}, in relation to anatomy and lesion identification, significantly higher mean classification values were obtained for both readers with ADC_{12} than with ADC_4 ($p < 0.001$), demonstrating that the proposed sequence with 12 b values provides a greater degree of sharpness than the standard sequence with 4 b values, both for evaluation of prostate anatomy and for characterization of suspicious lesions (Figures 7 and 8).

Interobserver agreement on classification of image quality and sharpness was measured by Kendall's Tau-b correlations, which revealed very strong agreement between the two readers regarding anatomical evaluation on both maps and evaluation of suspicious lesions in the ADC_{12} sequence (Tau-b> 0.9), as well as strong agreement for evaluation of suspicious lesions in the ADC_4 sequence (Tau-b = 0.836).

On the left (anatomical conspicuity) and on the right (lesion conspicuity), there is a predominance of high ratings from both readers for the ADC_{12} map. (Likert Scale from 2-5).

A and C, ADC_{12} sequence for characterization of a focal lesion (A) and anatomical aspects (C); B and D, ADC_4 sequence for characterization of the same focal lesion (B) and anatomical aspects (D).

Discussion

Diffusion sequences are well established in the literature as a key tool for prostate imaging, and diffusion findings are particularly recognized as a biomarker of tumor aggressiveness as assessed by mp-MRI [6-11]. The present study demonstrated the feasibility of DWI sequences with 12 b values in clinical practice, as compared to the standard (4 b values) ADC mapping used in mp-MRI.

Protocols with different b values have been studied in the recent literature [15-19], but there is still no established consensus as to the technical parameters of choice for mp-MRI of the prostate. Even the latest version of PI-RADS, published in 2015 and updated in 2019 (PI-RADS 2.1), doesn't come with the indication of how many b values should be used; it only recommends acquisition of a sequence with "ultra-high b values", which may add benefit in identification of lesions, but at the expense of decreased image sharpness [10,15,16]. In addition, other studies on diffusion sequences

Saad LS, et al., J Radiol Clin Imaging 2023
DOI:10.26502/jrci.2809067

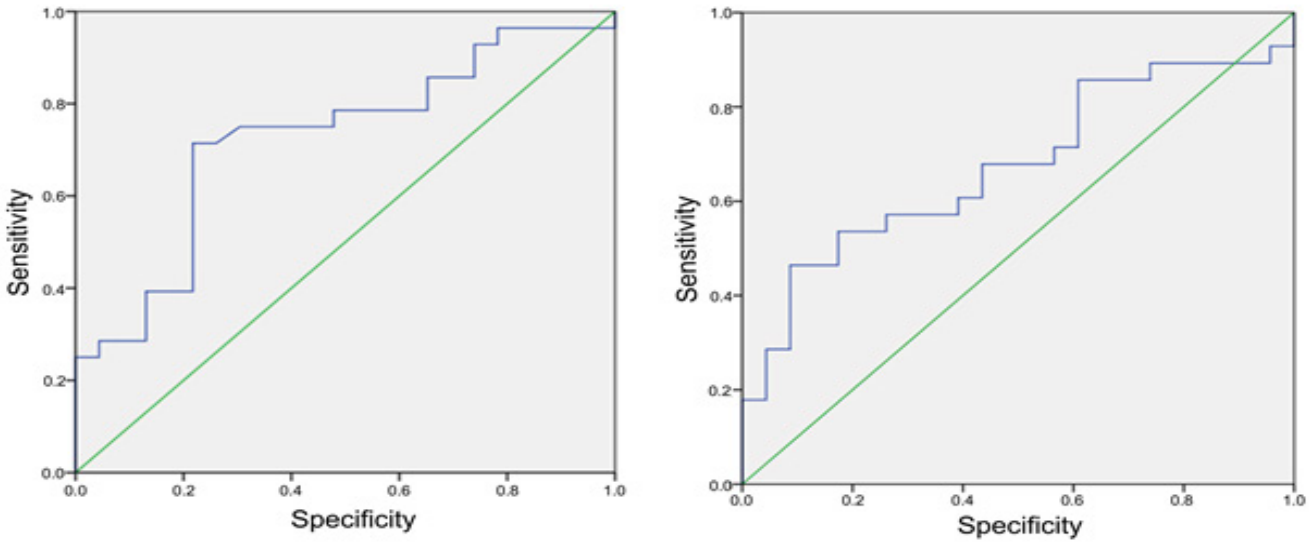

Figure 6: ROC curves for ADC_4 (left) and ADC_{12} (right). p <0.05.

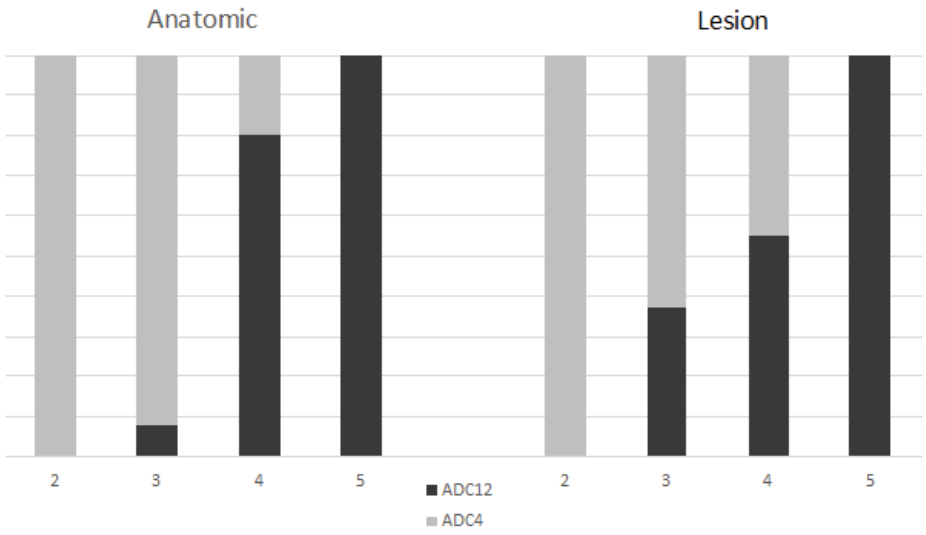

Figure 7: Diagram of image quality ratings for ADC_4 and ADC_{12} maps.
On the left (anatomical conspicuity) and on the right (lesion conspicuity), there is a predominance of high ratings from both readers for the ADC_{12} map. (Likert Scale from 2-5).

of the prostate have described an overlap between malignant neoplasms and benign focal lesions that restrict diffusion, such as benign prostatic hyperplasia nodules and focal areas of prostatitis [11-12].

Different models of b-value optimization for mp-MRI have also been studied, such as conducting a comparison between sequences to calculate ADC map to find out which combination is most useful to discriminate between low and high-grade neoplasms [18]. The overall image quality of ADC maps has been studied by testing combinations of paired b values [19]. Other more complex and refined techniques for calculating ADC, such as IVIM [20] and diffusion kurtosis [21], have been proposed as alternatives for imaging of prostate tissue, but there is still no established consensus for their routine use in the clinic.

In this case series, the aim was to improve the technical and image quality parameters of ADC maps while maintaining their high diagnostic utility.

As a primary result, it was observed that the conspicuity and sharpness of the images obtained by the ADC map with 12 b values was significantly greater than that obtained with 4 b values, both for evaluation of anatomy and for focal lesions. Thus, interpretation of the images for characterization of suspicious lesions was significantly improved, overcoming a challenge that is reported in the current literature. This improvement in image quality substantially helps optimize the prostate scanning protocol. With the recent trend in the literature of making MRI the imaging modality of choice for PCa screening, consequently increasing the importance of T2 and DWI sequences [22-23], and the progressive shift toward

Saad LS, et al., J Radiol Clin Imaging 2023
DOI:10.26502/jrci.2809067

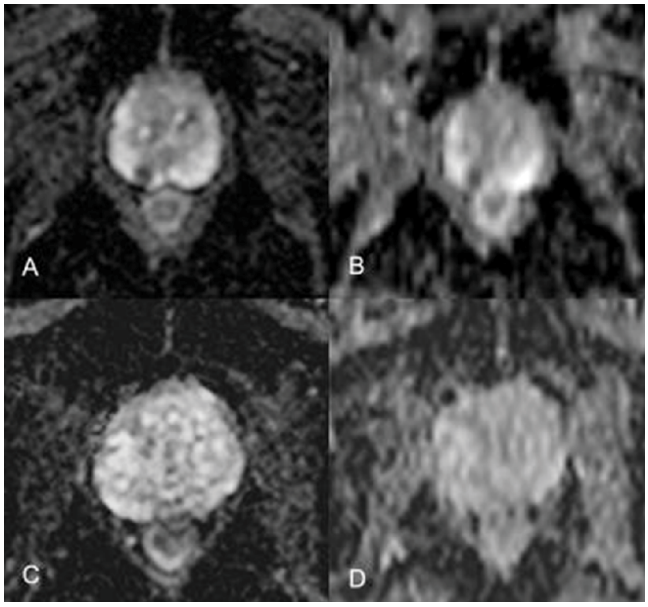

Figure 8. Comparison between image quality in ADC maps. A and C, ADC_{12} sequence for characterization of a focal lesion (A) and anatomical aspects (C); B and D, ADC_4 sequence for characterization of the same focal lesion (B) and anatomical aspects (D).

biparametric rather than mp-MRI protocols, this optimization should be of great value to make scans more effective in identifying suspicious lesions. Also considering the near future and likely introduction of artificial intelligence-based diagnostic algorithms for mp-MRI, improving the definition of images used to train such diagnostic programs may enhance their performance for identification of suspicious lesions.

As a secondary result, ADC measurements were lower in neoplastic tissue compared to normal prostate tissue, with statistically significant differences in both the standard (4 b value) and new (12 b value) techniques. In addition, ADC maps obtained with 12 b values were comparable to those of the sequence obtained with 4 values, both having a similar distribution among patients, and a constant ratio being obtained in both maps. On analysis of correlation with the PI-RADS classification, they effectively distinguished between lower-grade (3) and higher-grade (4 and 5) tumors and can thus be considered a useful parameter for assessing the aggressiveness of focal prostate lesions.

Although a statistically significant correlation of ADC_4 or ADC_{12} values with Gleason grade was not found, likely due to the small number of patients in whom histopathological examination of biopsy specimens was performed, mean absolute ADC values declined as the Gleason score rose, demonstrating that mean ADC values tend to correspond to tumor aggressiveness. Analysis of predictive value found that both sequences were good predictors of clinically significant cancer.

Major limitations of the present study include the technique of histopathological examination, which was performed on specimens obtained by cognitive fusion-targeted biopsy, while the gold-standard method for pathological study is prostatectomy. As a result, Gleason scores could have been different in some cases if specimens had been obtained by prostatectomy, thus changing the percentage of aggressive tumors. Another modality that is currently being studied and has shown promising results is MRI–ultrasound fusion biopsy of the prostate, which aids in adequate localization of the suspected lesion and allows collection of additional tissue fragments from the area that appears most abnormal on MRI [24-25]. Another limitation was the small number of patients whose biopsy was positive for prostate cancer (n=28), which is the probable cause of the limited statistical significance on comparison of ADC maps versus Gleason scores. It also bears stressing that, in clinical practice, there is a perception that positive biopsy results - especially with lower Gleason grades - may not correspond to a visible lesion on diffusion-weighted imaging. Therefore, a larger sample is needed, as well as further studies relating imaging techniques and biopsy findings with proven neoplasms, to adequately compare the diffusion sequence in mp-MRI with the anatomopathological results.

Conclusion

The present study sought to conduct a qualitative and quantitative evaluation of the use of an alternative to conventional diffusion sequences in mp-MRI of the prostate and analyze its possible implications in the diagnosis of PCa by magnetic resonance imaging.

The new technique using 12 b values was compared to the standard sequence already made (using 4 b values) regarding image quality, as well as a quantitative comparison by ADC measurement. Other validated comparison parameters were also used, such as the PI-RADS scale and the Gleason score, both of which perform well and are widely accepted and used in clinical practice by radiologists and urologists alike.

The conclusion is that a diffusion sequence with 12 b values is perfectly feasible for MRI study of the prostate, and that it provides superior image quality and clarity as compared to current techniques. It demonstrated a constant relationship with standard diffusion and superior anatomical definition, in addition to good correlation with the PI-RADS classification and with Gleason score, thus validating its clinical use.

References

1. Sung H, Ferlay J, Siegel RL, et al. Global cancer statistics 2020: GLOBOCAN estimates of incidence and mortality worldwide for 36 cancers in 185 countries. CA Cancer J Clin 71 (2021): 209- 249.
2. Steyn JH, Smith FW. Nuclear magnetic resonance imaging of the prostate. Br J Urol 54 (1982): 726-728.
3. Poon PY, McCallum RW, Henkelman MM, et al.Magnetic

resonance imaging of the prostate. Radiology 154 (1985): 143-149.

4. Barentsz JO, Richenberg J, Clements R, et al. Radiology ESoU. ESUR prostate MR guidelines Eur Radiol 22 (2012): 746-757.

5. American College of Radiology. Prostate Imaging Reporting and Data System (PI-RADS). 76(3) (2019): 340-351.

6. Rosenkrantz AB, Parikh N, Kierans AS, et al. Prostate Cancer Detection Using Computed Very High b-value Diffusion-weighted Imaging: How High Should We Go? Acad Radiol 23 (2016): 704-711.

7. Padhani AR, Liu G, Koh DM, et al. Diffusion-weighted magnetic resonance imaging as a cancer biomarker: consensus and recommendations. Neoplasia 11 (2009): 102-125.

8. Anwar SS, Anwar Khan Z, Shoaib Hamid R, et al. Assessment of apparent diffusion coefficient values as predictor of aggressiveness in peripheral zone prostate cancer: comparison with Gleason score. ISRN Radiol 9 (2014).

9. Hambrock T, Somford DM, Huisman HJ, et al. Relationship between apparent diffusion coefficients at 3.0-T MR imaging and Gleason grade in peripheral zone prostate cancer. Radiology 259 (2011): 453-461.

10. Tamada T, Kanomata N, Sone T, et al. High b value (2,000 s/mm2) diffusion-weighted magnetic resonance imaging in prostate cancer at 3 Tesla: comparison with 1,000 s/mm2 for tumor conspicuity and discrimination of aggressiveness PLoS One 9 (2014): e96619.

11. El Kady RM, Choudhary AK, Tappouni R. Accuracy of apparent diffusion coefficient value measurement on PACS workstation: A comparative analysis. AJR Am J Roentgenol 196 (2011): 280-284.

12. Hoeks CM, Vos EK, Bomers JG, et al. Diffusion-weighted magnetic resonance imaging in the prostate transition zone: histopathological validation using magnetic resonance-guided biopsy specimens. Invest Radiol 48 (2013): 693-701.

13. Metens T, Miranda D, Absil J, et al. What is the optimal b value in diffusion-weighted MR imaging to depict prostate cancer at 3T? Eur Radiol 22 (2012): 703-709.

14. Manenti G, Nezzo M, Chegai F, et al. DWI of Prostate Cancer: Optimal b-Value in Clinical Practice. Prostate Cancer 4(2014).

15. Kitajima K, Takahashi S, Ueno Y, et al. Clinical utility of apparent diffusion coefficient values obtained using high b-value when diagnosing prostate cancer using 3 tesla MRI: comparison between ultra-high b-value (2000 s/mm²) and standard high b-value (1000 s/mm²). J Magn Reson Imaging 36 (2012): 198-205.

16. Grant KB, Agarwal HK, Shih JH, et al. Comparison of calculated and acquired high b value diffusion-weighted imaging in prostate cancer. Abdom Imaging 40 (2015): 578-586.

17. Bittencourt LK, Attenberger UI, Lima D, et al. Feasibility study of computed vs measured high b-value (1400 s/mm²) diffusion-weighted MR images of the prostate. World J Radiol 6 (2014): 374-380.

18. Hurrell SL, McGarry SD, Kaczmarowski A, et al. Optimized b-value selection for the discrimination of prostate cancer grades, including the cribriform pattern, using diffusion weighted imaging. J Med Imaging (Bellingham) 5(2018): 011004.

19. Xi Y, Liu A, Olumba F, et al. Low-to-high b value DWI ratio approaches in multiparametric MRI of the prostate: feasibility, optimal combination of b values, and comparison with ADC maps for the visual presentation of prostate cancer. Quant Imaging Med Surg 8(2018): 557-567.

20. Pang Y, Turkbey B, Bernardo M, et al. Intravoxel incoherent motion MR imaging for prostate cancer: an evaluation of perfusion fraction and diffusion coefficient derived from different b-value combinations. Magn Reson Med 69(2) (2013): 553-562.

21. Rosenkrantz AB, Sigmund EE, Johnson G, et al. Prostate cancer: feasibility and preliminary experience of a diffusional kurtosis model for detection and assessment of aggressiveness of peripheral zone cancer. Radiology 264(1) (2016): 126-135.

22. Barth BK, De Visschere PJL, Cornelius A, et al. Detection of Clinically Significant Prostate Cancer: Short Dual-Pulse Sequence versus Standard Multiparametric MR Imaging-A Multireader Study Radiology 28 (3) (2017): 725-736.

23. Kuhl CK, Bruhn R, Krämer N, et al . Abbreviated Biparametric Prostate MR Imaging in Men with Elevated Prostate-specific Antigen. Radiology 285(2) (2017): 493-505.

24. Ahmed HU, El-Shater Bosaily A, Brown LC, et al. Diagnostic accuracy of multi-parametric MRI and TRUS biopsy in prostate cancer (PROMIS): a paired validating confirmatory study. Lancet 389(10071) (2017): 815-822.

25. Mariotti GC, Costa DN, Pedrosa I, et al . Magnetic resonance/transrectal ultrasound fusion biopsy of the prostate compared to systematic 12-core biopsy for the diagnosis and characterization of prostate cancer: multi-institutional retrospective analysis of 389 patients. Urol Oncol 34(9) (2016): 416